8-1-2010

Imaging of vibrating objects using speckle subtraction

Thomas R. Moore
TMOORE@rollins.edu

Ashley E. Cannaday

Sarah A. Zietlow
Department of Physics, Rollins College

Published In

Thomas R. Moore, Ashley E. Cannaday, and Sarah A. Zietlow, "Imaging of vibrating objects using speckle subtraction," J. Opt. Soc. Am. A 27, 1863-1867 (2010)

Imaging of vibrating objects using speckle subtraction

Thomas R. Moore,[1,*] Ashley E. Cannaday,[1] and Sarah A. Zietlow[2]

[1]*Department of Physics, Rollins College, Winter Park, Florida 32789, USA*
[2]*Paul J. Hagerty High School, Oviedo, Florida 32765, USA*
[*]*Corresponding author: tmoore@rollins.edu*

Received April 20, 2010; revised June 16, 2010; accepted July 1, 2010;
posted July 6, 2010 (Doc. ID 127192); published July 28, 2010

A simple method for imaging vibrational motion is proposed. The process consists of capturing two speckled images of a region illuminated by coherent radiation. One of the images is captured before the onset of motion and the other during motion. If the mean speckle intensity is below the threshold for detection or above the saturation intensity of the detector, subtracting the two images produces a high contrast image of the moving region. A theory is shown to agree well with experimental data. © 2010 Optical Society of America

OCIS codes: 120.7280, 120.6150, 110.6150.

1. INTRODUCTION

The scientific and engineering communities have been interested in imaging small vibrations since the 18th century, when Chladni first placed sand on a vibrating plate to make the modal patterns visible. Other methods were developed in the latter half of the 20th century that made it possible to optically image sub-micrometer vibrations, including laser Doppler vibrometry, holographic interferometry, and electronic speckle pattern interferometry [1]. Each of these methods is still in common use today, and they have found wide application in situations requiring visualization of small-amplitude motion. Unfortunately, each of these processes requires expensive equipment and usually requires isolating the object of interest from ambient vibrations. Laser speckle contrast analysis (LASCA) overcomes these problems by calculating the difference in speckle contrast that results from the relative motion of different parts of an imaged area, and it can be used in some cases to differentiate between moving and non-moving regions in an image [2,3]. However, while LASCA does not require an extensive investment in equipment, it does require significant image processing and the resolution of the resulting image is at best 25% that of the resolution of the detector.

Here we introduce another method of visualizing vibrations that fundamentally differs from those mentioned above. This method provides large-area imaging of micrometer-sized motion in real time without the need for expensive equipment, extensive signal processing, or isolating the object from ambient vibrations. The necessary condition to apply this method is that the motion of the object of interest can be induced on a time scale that is shorter than that which characterizes the ambient motion. Surprisingly, this requirement is met in many instances where the more common methods of detecting vibrations do not work well. We have tentatively termed the process speckle subtraction imaging (SSI).

To image vibrations using speckle subtraction imaging, the area of interest must be illuminated by light with a narrow enough linewidth that the speckle pattern that results from imaging the area of interest has a high contrast. The region of interest is then imaged onto a detector and two images are captured. One image is captured while the motion of interest is ongoing, and the other is captured either before the motion begins or after it has stopped. The two images are then subtracted in real time to produce a difference image. As expected, subtracting two images of the region will produce a completely black difference image in regions where no motion was induced. However, since some motion in the imaged area was induced during the process of capturing one of the images, the portion subject to motion will produce a speckle pattern with lower contrast than will be seen in regions that were not moving.

This reasoning may lead one to believe that merely imaging an area that is illuminated by coherent radiation and subtracting subsequent images captured before and after the onset of motion will result in areas of motion being visible in the image. Unfortunately, this is not generally the case because ambient motion usually changes the speckle pattern slightly during the time needed to record the two images, or the speckle is not completely resolved on the detector. Since the mean value of the speckle intensity does not normally change with induced motion, either of these situations will result in an inability to easily differentiate between moving and non-moving regions.

One way to take advantage of the change in the speckle contrast to unambiguously detect motion within the imaged area is to introduce a nonlinearity into the detection process. In speckle subtraction imaging, it is the fact that all detectors have a minimum intensity below which they will not record the image that allows regions of motion to become visible. A detection threshold is a characteristic of all detectors, so it is not necessary to specify the type of detector *a priori*.

When the mean intensity of the speckle is below the

threshold for detection (or above the saturation intensity), only speckle with an intensity that is in the tail of the intensity distribution will be detected. Since a reduction in speckle contrast occurs when the imaged object is set into motion, because of a reduction in the standard deviation of the intensity distribution, a change in speckle contrast will result in a change in the mean detected intensity. This will occur even though the mean intensity of the speckle does not change. Therefore, subtracting an image with little motion on the time scale of the integration time of the detector from one where some portion of the image is moving during the collection process will result in an image that differentiates the moving portion by a measurable change in the recorded intensity. In this way, areas of little motion (high speckle contrast) can be differentiated from areas where motion occurs (low speckle contrast) with only minimal signal processing.

2. THEORY

To investigate the process of SSI theoretically we introduce two correlation times. We refer to the correlation time of light scattered from the region during the induced motion as τ_1, and the longer correlation time that is measured either before the motion has begun or after it has ceased as τ_2. The speckle contrast K_1 and K_2 will be different for the two cases, but the mean intensity of the speckle $\langle I\rangle$ will be the same. The contrast is defined as

$$K=\frac{\sigma}{\langle I\rangle}, \tag{1}$$

where σ represents the standard deviation of the intensity distribution; therefore, in the case considered here the contrast is linearly proportional to σ.

If the mean value of the speckle intensity is below the threshold for detection, simply subtracting two images will produce an image with nonzero intensity if the statistics of the scattered light have changed between the two images. Defining the integration time of the detector as T and the time between capturing the two images as Δt, and assuming that $2T+\Delta t \ll \tau_2$, the speckle pattern from the region where no motion was induced will not change significantly between the time that the two images are captured. This condition implies that if there is no onset of motion between two images then they are identical, and the subtraction process will result in a new image with no variation in intensity.

The intensity of any region of interest that is imaged onto a detector can be approximated by the mean value of the speckle intensity, which is defined as usual by

$$\langle I\rangle=\int_0^\infty IP(I)dI, \tag{2}$$

where $P(I)$ is the probability density function for the intensity and I is the intensity. The probability density function for the intensity of fully developed speckle of finite bandwith can be written in terms of the speckle contrast, and this can be used to approximate the probability density in the case considered here. In its approximate form this function is [4]

$$P_M(I)=\frac{(M)^M I^{M-1}}{\langle I\rangle^M \Gamma(M)} e^{-MI/\langle I\rangle}, \tag{3}$$

where $\Gamma(M)$ is the gamma function with argument M, and $M=K^{-2}$.

As noted above, since the mean intensity of fully developed speckle will be the same for all values of M, calculating the mean value of the speckle intensity of the region will result in the same value regardless of the correlation time of the scattered light. In this case a region that is in motion will not contrast sharply with the other areas of the image. However, the detector does not have an infinite response; therefore, the limits of integration in Eq. (2) do not extend from zero to infinity if one wishes to calculate the mean value of the intensity recorded by the detector. Rather, the intensity measured by the detector is calculated by assuming a lower limit that has some value, I_L, that is greater than zero. All detectors also have a saturation intensity, so the upper limit of the integration must be some value, I_U, that is less than infinity. Therefore, while the mean value of the speckle incident on the detector is given by Eq. (2), the value that is recorded by the detector is not.

The intensity of the SSI image, which results from taking the absolute value of the difference between two images of the same area with different scattering statistics, is given by

$$\begin{aligned} I_{SSI}(M_1,M_2)=\Bigg|&\left\{\int_{I_L}^{I_U}(I-I_L)P_{M_1}(I)dI+\int_{I_U}^{\infty}(I_U)P_{M_1}(I)dI\right\}\\ &-\left\{\int_{I_L}^{I_U}(I-I_L)P_{M_2}(I)dI\right.\\ &\left.+\int_{I_U}^{\infty}(I_U)P_{M_2}(I)dI\right\}\Bigg|, \end{aligned} \tag{4}$$

where $M_n=K_n^{-2}$ and n is either 1 or 2 depending on which case is under consideration. More succinctly, Eq. (4) can be written as

$$\begin{aligned} I_{SSI}(M_1,M_2)=\Bigg|&\int_{I_L}^{I_U}(I-I_L)\{P_{M_1}(I)-P_{M_2}(I)\}dI\\ &+(I_U)\int_{I_U}^{\infty}\{P_{M_1}(I)-P_{M_2}(I)\}dI\Bigg|. \end{aligned} \tag{5}$$

If the mean value of the speckle intensity falls between I_L and I_U, the effect of having a threshold of detection and a saturation intensity will be minimal. However, if $\langle I\rangle < I_L$, then when $M_1\neq M_2$ the result will be that $I_{SSI}(M_1,M_2)>0$. A plot of the mean recorded intensity as a function of speckle contrast is shown in Fig. 1 for three different values of I_L. One can conceivably pick any value of I_L to achieve the desired slope of image intensity versus speckle contrast; however, if $\langle I\rangle \ll I_L$ the number of speckles with a detectable intensity becomes vanishingly small. In practice, the second term in Eq. (5) can usually be ignored and the intensity of the SSI image can be expressed as

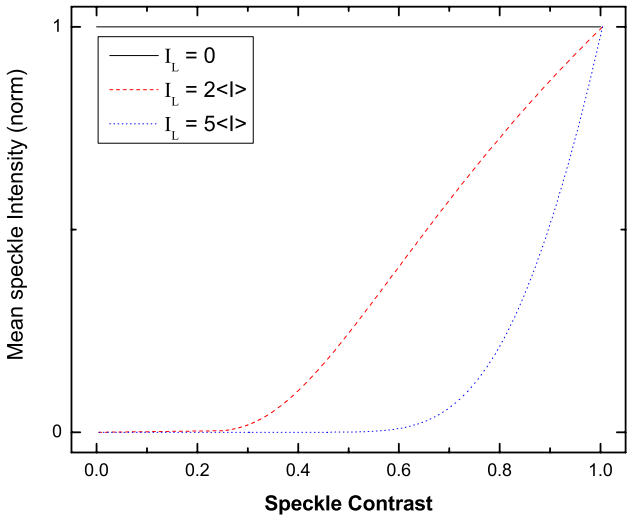

Fig. 1. (Color online) Plot of the mean recorded intensity of the speckle as a function of speckle contrast predicted by Eq. (5) for three different values of the detector threshold.

$$I_{SSI}(M_1,M_2) \approx \left| \int_{I_L}^{I_U} (I - I_L)\{P_{M_1}(I) - P_{M_2}(I)\} dI \right|. \quad (6)$$

A similar analysis can be performed for the case where $\langle I \rangle > I_U$.

To theoretically investigate the utility of SSI in imaging vibrations, it is useful to assume a probability density function that represents a common situation. Therefore, we assume that the area being imaged consists of a large number of independent particles, and that the incident light is scattered randomly from numerous particles before being detected. In this case the instantaneous field is a complex circular Gaussian process. We further assume that at some point in time the motion of the particles can be induced, and that the motion of these particles at that time can be described as being stochastic. This situation has been studied by Duncan and Kirkpatrick, who have shown that the speckle contrast of the scattered light is given by [2]

$$K_n = \sqrt{\gamma_n - \frac{\gamma_n^2}{2}(1 - e^{-2/\gamma_n})}, \quad (7)$$

where the normalized correlation time is defined as

$$\gamma_n = \frac{\tau_n}{T}. \quad (8)$$

In practice, it is the visibility of the moving region with respect to a non-moving region that is of interest. The visibility is defined as

$$V = \left| \frac{I_1 - I_2}{I_1 + I_2} \right|, \quad (9)$$

where I_1 and I_2 are the intensities of the SSI image in the areas that represent the moving and static regions, respectively. That is, $I_1 = I_{SSI}(M_1,M_2)$ and $I_2 = I_{SSI}(M_2,M_2)$. It is evident that the visibility of the part of an SSI image that is in motion is always unity provided $\gamma_1 < \gamma_2$, because I_2 is always identically zero. Unfortunately, this is only true in practice if $\frac{2T+\Delta t}{\tau_2} \gg 1$. While this can be arranged in some cases, it is more instructive to assume that there is some minimal change in the speckle over the time $2T + \Delta t$ that does not result in a change in the contrast or the mean recorded intensity, but will generally result in changes in the details of the speckle. This change can usually be attributed to ambient motion. In this case the point by point subtraction of the two images will result in I_2 having some small, non-zero value.

For the purpose of theoretically investigating the visibility of an SSI image, we will assume that in the absence of any induced motion in the region, the SSI process produces an image with an average intensity on the order of one-tenth the mean value recorded by the detector before subtraction. This value appears consistent with the experiments described below. The visibility of SSI as a function of γ_1 is plotted for several different values of γ_2 in Fig. 2 using this assumption. The threshold for detection is assumed to be twice the value of the mean intensity of the speckle.

There are two surprising conclusions that can be drawn from the results shown in Fig. 2. First, the shape of the curves indicates that regions of motion will be visible in the SSI image even when the value of γ_1 approaches that of γ_2. There is a nonlinear relationship between the visibility and γ_1, but the visibility remains high until $\gamma_1 \sim \gamma_2$. The second interesting result is that it is possible to detect the motion of an object using SSI even when there is significant ambient motion. Even when the integration time of the detector is twice the correlation time of the light scattered from the region with no induced motion (i.e., $\gamma_2 = 0.5$), the visibility of a moving region within an SSI image can be as high as 0.5.

3. EXPERIMENTS

To demonstrate that the theory described above accurately describes the process of SSI, a 2 cm diameter piezoelectric disk was covered with approximately 0.5 cm of fine sand. The surface of the sand was illuminated with light from a laser with variable output power having a wavelength of 532 nm, and the image was projected onto a CCD array using a commercially available camera lens. The integration time of the array was specified by the manufacturer as being 0.0313 s. The piezoelectric disk was driven by a 295 Hz sinusoidal signal with an amplitude that varied from 0–10 V. The light from the laser was expanded using a short focal length lens and projected onto the area at an angle of approximately 10°. The area of interest was imaged from directly above; however, there were no discernible effects attributable to imaging the area at an oblique angle, except for the fact that the area of interest covered a smaller region on the detector.

To ensure maximum contrast, the mean diameter of the speckle was chosen to be close to the pixel size of the digitized image, which corresponded to approximately 13 μm on the CCD array. The mean speckle diameter on the array is given by

$$d = 1.22(1 + m)\lambda f, \quad (10)$$

where m is the magnification of the image, λ is the wavelength of the light, and f is the aperture ratio of the im-

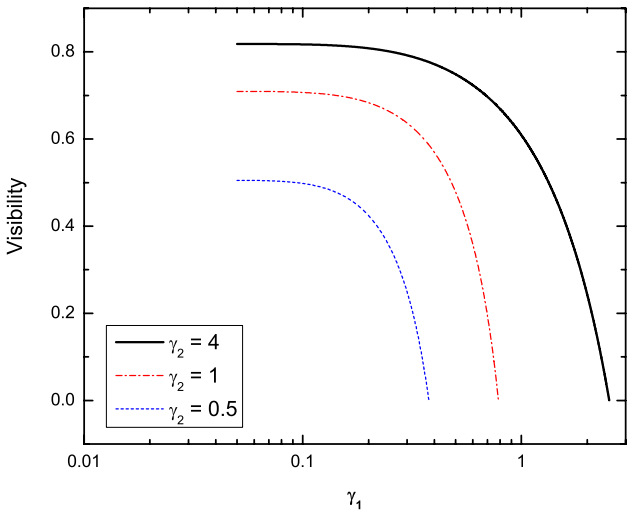

Fig. 2. (Color online) Plot of the visibility of SSI as a function of γ_1 for three different values of γ_2. The threshold for detection is assumed to be twice the mean intensity of the speckle ($I_L=2\langle I\rangle$).

aging lens. The calculated speckle size was approximately 12 μm.

The amplitude of the oscillation of the piezoelectric disk as a function of driving potential was determined beforehand by viewing the disk through an electronic speckle pattern interferometer while it was driven with a sinusoidal signal of several different amplitudes. Measurements of the amplitude of oscillation were recorded as a function of driving voltage, and a linear regression of the data revealed the slope to be 297±6 nm/V. In all cases the light reaching the detector was from the surface of the sand, not the piezoelectric disk, and although the driving motion was harmonic it is reasonable to expect that on average the motion of the top region of the sand can be approximated as Brownian.

The decay time of the motion of the sand was measured by recording the speckle pattern reflected from the area with a high-speed camera having a frame rate of 1 kHz. The individual images were studied to determine how long it took for the speckle pattern to become static after the piezoelectric disk stopped moving. The motion of the sand ceased within 8±1 ms. The time between capture of the two images was approximately 300 ms, ensuring that images taken after the motion had stopped did not exhibit the effects of residual motion of the sand.

In each experiment an image of the surface of the sand was stored before the piezoelectric disk was activated. Another image was captured after the disk began to vibrate. The mean and standard deviation of the intensity of the region was calculated for each case (before motion, during motion, and after image subtraction) and stored for later analysis. The region used for analysis encompassed approximately 57,000 pixels and the results from 50 images were averaged for each different value of the driving potential.

Once the data had been collected, the visibility of the SSI image for each driving potential was calculated using Eq. (9). The intensity I_2 was derived from the SSI image obtained by subtracting two different images of the region with no induced motion. The intensity I_1 in each case was the average of the SSI intensity in the region that resulted from subtracting an image captured during the time that the motion was induced from one captured during a time with no induced motion. The speckle contrast recorded by the detector, which is defined by Eq. (1), was also calculated for each driving potential. Using the same region to determine both I_1 and I_2, rather than using separate moving and non-moving regions in a single image, eliminated the effects attributable to uneven illumination and ensured that the true value of the visibility was measured.

The results of these experiments are plotted in Fig. 3 along with the predictions derived from Eq. (5) using the probability density function shown in Eq. (3). The only free parameter in the fitting process was the ratio of the threshold intensity I_L to the mean value of the speckle intensity $\langle I\rangle$.

Note that to effectively apply SSI to the study of vibrating objects it is not necessary to know the statistics of the speckle. All that is required to image a vibrating region in an image is that the contrast of the speckle change when the object being imaged is set into motion. Therefore, SSI

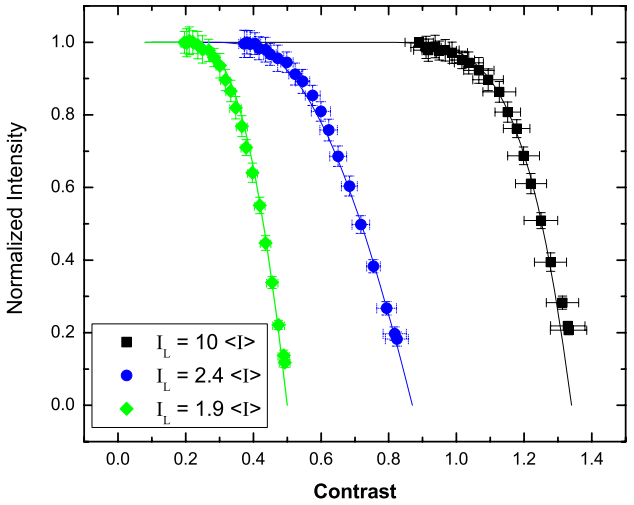

Fig. 3. (Color online) Plot of the normalized intensity of SSI image as a function of contrast for three different threshold values. The curves represent the predictions of Eq. (5).

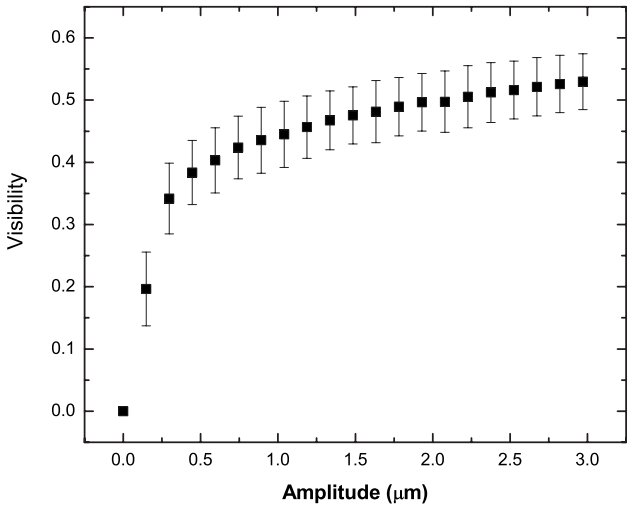

Fig. 4. Plot of the visibility of the piezoelectric disk as a function of the amplitude of vibration.

can be used in many situations for detection and analysis of vibrations. To demonstrate this, the sand was removed from above the piezoelectric disk, which was then painted white. The visibility of the vibrating surface alone was measured and is plotted as a function of amplitude of vibration in Fig. 4.

4. CONCLUSIONS

The data presented above indicate that speckle subtraction imaging may be useful in situations where imaging vibrations is necessary, but the more common imaging techniques are difficult to implement. As can be seen in Fig. 2, the integration time of the detector can exceed the decorrelation time attributable to ambient motion by as much as a factor of two and still result in high visibility. In the experiments reported here, no effort was made to control the integration time of the detector. However, the addition of a camera with a variable integration time will provide considerable flexibility in controlling the normalized correlation times γ, and will expand the applicability significantly.

Speckle subtraction imaging is a simple, inexpensive method that requires minimal equipment and limited experience to implement. Yet it can provide high-resolution images of micrometer-sized motion of objects under a wide variety of conditions in near real time. Although SSI does not provide a precise measurement of the amplitude of vibration, the visibility provides an estimate of the amplitude. Furthermore, the motion under study need not be continuous or harmonic, and therefore SSI can be used to image transient motion and differential flow.

ACKNOWLEDGMENTS

This work was supported by National Science Foundation (NSF) grant no.0551310 and the generosity of Christine Lenore Barensfeld.

REFERENCES

1. N.-E. Molin, "Optical methods for acoustics and vibration measurements," in *Handbook of Acoustics*, T. Rossing, ed. (Springer, 2007), pp. 1101–1123.
2. D. D. Duncan and S. J. Kirkpatrick, "Can laser speckle flowmetry be made a quantitative tool?" J. Opt. Soc. Am. A **25**, 2088–2094 (2008).
3. A. R. Fercher, "Velocity measurement by first order statistics of time-differentiated laser speckles," Opt. Commun. **33**, 129–135 (1980).
4. G. Parry, "Speckle patterns in partially coherent light," in *Laser Speckle and Related Phenomena*, J. C. Dainty, ed. (Springer, 1984), pp. 77–122.